

Picosecond Studies of Nonequilibrium Flux Dynamics in a Superconductor

M. R. Freeman

IBM Thomas J. Watson Research Center, Yorktown Heights, New York 10598

(Received 13 May 1992)

A fast magneto-optical technique is used to explore flux dynamics in the optically driven nonequilibrium state of type-I superconducting Pb films. It is found that the penetration of magnetic flux through the nonequilibrium intermediate state can be dramatically *faster* than through the normal metal. Studies as a function of how far the system is driven from equilibrium, and of the effect of a static applied magnetic field, indicate that the observations reflect the dynamics of normal/superconducting interfaces, and are strongly dependent on the microscopic pattern of the intermediate state.

PACS numbers: 74.30.Gn, 74.40.+k, 74.75.+t, 78.47.+p

The behavior of magnetic flux threading superconducting specimens has been a topic of continuing interest for several decades, during which time a rich variety of phenomena have been elucidated owing to the diversity of intrinsic and extrinsic characteristics of these materials [1]. Direct measurements of flux penetration rates through superconductors have characteristically been performed only on relatively long (\geq ms) time scales [2], limited by the large length scales on which the flux motion has been studied, and by pinning effects. Recent theories of the kinetics of the superconducting transition demonstrate, however, that the intrinsic flux dynamics on a local scale proceed on ultrashort time scales [3]. It is of great interest to access this regime experimentally with a flux-sensitive probe combining high temporal and spatial resolution, and to explore how the microscopic pattern of normal/superconducting (N/S) interfaces influences the dynamics. Furthermore, improved time resolution would enable direct studies of flux dynamics in a new regime, that of a thin-film superconductor in the intermediate state, driven out of equilibrium by electron heating from transient optical excitation [4]. An electron heating pulse could affect the dynamics in two major ways: by setting N/S interfaces in motion in the nonequilibrium regime [5] and thereby overcoming the static flux friction barrier, and by breaking superconducting paths between isolated islands of normal region in which flux changes would otherwise be prevented by quantization.

In this work we report time-domain studies of flux dynamics in the nonequilibrium state of high-purity Pb thin films, using novel magneto-optical techniques that allow investigations on these very short time scales [6,7]. Pb was chosen for these studies because, among the type-I superconductors, it is the most favorable system for optically driven electron heating, and furthermore has been the most extensively characterized by other methods. Here the dynamics of N/S interfaces are effectively probed on a local scale by coupling to their motion with picosecond rise-time pulsed magnetic fields. The interface velocity is dependent in part on the normal-state conductivity, which influences the rate at which energy is dissipated near a moving N/S interface [8]. The relevant *local* conductivity is determined here by a direct measurement of the diffusion constant of the magnetic field in

the normal metal.

These experiments reveal new information about the dynamics of the nonequilibrium superconducting state. In contrast to the conventional screening behavior of a superconductor [9], and to an expectation based on the lower-than-normal resistivity observed in the nonequilibrium regime by transport measurements [10–12], it is found here that *faster* penetration of magnetic flux can occur in the nonequilibrium regime than when the metal is in the normal state. This phenomenon is strongly dependent on the applied static field and on the degree to which the system is driven from equilibrium by optical excitation. It is suggested that these dependencies are manifestations of the microscopic pattern of normal/superconducting interfaces in the intermediate state. Qualitatively, the time scale for flux penetration will decrease as the pattern of the intermediate state becomes more convoluted, both because a greater total length of N/S interface within a given area requires smaller displacements to accommodate a change of applied field, and because the local interface velocity increases with increasing curvature.

Experimentally, the requisite high temporal resolution is obtained through the use of fast magneto-optic sensors and lithographically patterned pulsed-field coils, as schematically illustrated in the inset to Fig. 1. A 2-mm-diam superconducting sample film, thermally evaporated from 99.9999% Pb onto a thin glass substrate, is sandwiched between a 500- μ m-diam pulsed-field coil on a silicon substrate (providing a transient magnetic field normal to the surface) and a 120-nm-thick EuS(10% BaF₂) magneto-optic sensor film on fused quartz. The resulting stack is cooled in a 0–7-T split-coil magneto-optic Dewar. Pb films ranging in thickness from 100 nm to 1.2 μ m are studied here; these are characteristically type I as has been determined by direct observations of the intermediate state in decoration experiments [13]. Local changes in flux density are recorded by the polarization (Faraday) rotation on reflection from the sensor [14] of a weak (average power $<$ 100 μ W) focused optical probe beam consisting of 3-ps-wide pulses delivered by a dye laser cavity dumped at 19 kHz. The fundamental time resolution of this stroboscopic scheme is limited by the spin-lattice relaxation time in the sensor films [7], which

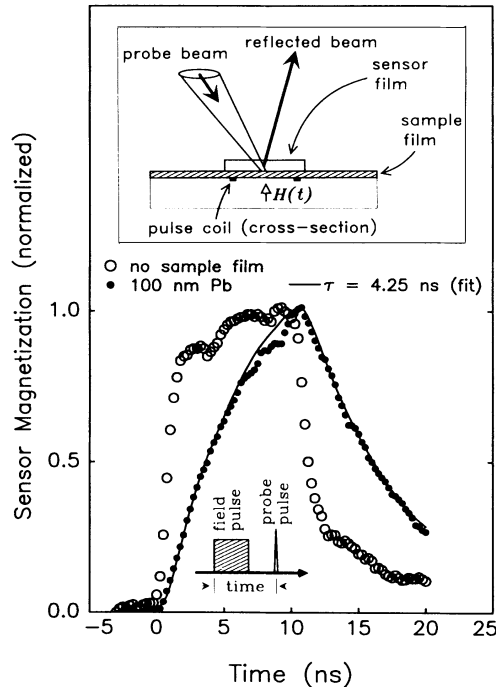


FIG. 1. The temporal response of a 120-nm EuS(10% BaF₂) sensor to a 10-ns duration magnetic field pulse, plotted as a function of optical probe delay (open circles). The solid circles show a time-domain screening measurement for a 100-nm normal Pb film ($H_0=1000$ Oe, $T=1.5$ K). The solid line is a fit and yields a single exponential time constant. Inset: Experimental geometry, where $H(T)$ is the pulsed field.

here is of order 100 ps. The arrival time of the magnetic field pulses is electronically controlled with an accuracy of 5 ps. In the absence of optically induced nonequilibrium effects, the present measurements are analogous to two-coil mutual inductance experiments on thin-film superconductors [15], albeit extended to ultrafast time scales and with the possibility of local spatial probing on a scale comparable to that of the flux structures. The open symbols in Fig. 1 show a system calibration with the Pb film removed, for a 10-ns duration, 30-Oe amplitude magnetic field pulse, plotted as a function of the optical probe delay relative to the onset of the field pulse (the pulse sequence is illustrated in the lower part of Fig. 1). The sensor reflection is enhanced by a semitransparent ($\approx 20\%$) 30-nm Au film, which also eliminates the possibility of exchange coupling between the Pb and the EuS when the films are stacked. Control measurements have been made with a fully opaque dirty Al reflector layer, in which case no optically induced nonequilibrium effects are observed.

The Pb films are initially characterized by low-frequency (15.9 Hz) magnetotransport measurements on meander lines simultaneously deposited on the same substrates as the actual screening films. These results yield nearly bulklike critical fields (800 Oe) and temperatures (7.2 K). Further characterization of the films comes

from the dynamic screening response of the normal metal. This is shown by the solid circles in Fig. 1 for a 100-nm normal Pb film ($T=1.5$ K, $H=1000$ Oe; within the accuracy of the measurements, the screening response is independent of field for $H > H_c$), measured using the same 10-ns duration field pulse. Screening by exponentially decaying eddy currents in the sample film transforms the system response to an arbitrary transient magnetic field $H(t)$, such that the sensor magnetization $M(t)$, proportional to the change in penetrating flux density, is described by

$$M(t) = \chi \frac{e^{-t/\tau}}{\tau} \int_0^t H(t') e^{t'/\tau} dt',$$

where χ is the magnetic susceptibility of the sensor film. The solid line in the lower part of Fig. 1 is a fit based on the unscreened $H(t)$, which are shown by the open circles, and yields the exponential time constant, $\tau = 4.25$ ns. τ then determines the diffusion constant for the magnetic field, $D_B = d^2/\tau$, where d is the film thickness. The numerical value of D_B for the 100-nm Pb film whose response is depicted by the solid circles in Fig. 1 is $2.4 \times 10^{-6} \text{ m}^2 \text{ s}^{-1}$, which corresponds, through $D_B = c^2/4\pi\sigma_n$, to a normal-state conductivity $\sigma_n = 3.3 \times 10^9 \text{ } \Omega^{-1} \text{ cm}^{-1}$ at $T=1.5$ K. This is $70000\times$ higher than the room-temperature conductivity, a remarkable ratio for such a thin film, but observed here because, on the short time scale of the measurements, only length scales less than the dominant grain size are probed. It is found that $\tau \propto d^2$ at least up to 500 nm (within the scatter introduced by determination of the film thickness and run-to-run variations in sample purity), beyond which grain boundary dissipation can no longer be neglected.

When the static magnetic field is lowered and the Pb becomes superconducting, a "conventional" superconducting screening response is observed; that is, the penetrating flux signal vanishes. However, if the superconductivity is weakened or destroyed by electron heating from an optical prepulse (referred to below as the pump, and derived from the same beam and focused to the same spot as the probe) it is found that there is another time constant governing the rate of flux penetration in the nonequilibrium regime. This is illustrated in Fig. 2 for a thicker, 500-nm Pb film at several values of the applied static field H_0 ($T=1.5$ K). For simplicity, the final change in penetrating flux density (after the system has returned to equilibrium as determined by probe delay time independence) is shown as a function of the arrival time of the pump pulse relative to the onset of the field pulse (see the schematic illustration of the pulse sequence in Fig. 2). Plotted in this manner, the rising signal before $t=0$ reflects the effective time constant for flux penetration through the film in the nonequilibrium state. This time constant is much shorter than the diffusion time of the magnetic field through the normal metal [the comparison measurement is shown in Fig. 2(c)], and therefore must arise from a different mechanism, specifically

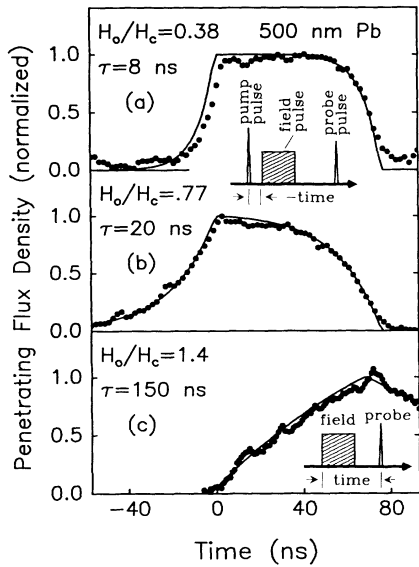


FIG. 2. (a),(b) The screening response of a 500-nm Pb film in the nonequilibrium regime to 71-ns-duration field pulses for two values of the reduced static applied field, plotted as a function of the time of arrival of the pump pulse driving the sample out of equilibrium with an absorbed energy density of 20 mJ/cm^3 . The solid lines are fits determining the time constant for flux penetration. (c) The normal-state screening response, for comparison. The schematics illustrate the pulse sequences and time variables used for the abscissa.

through coupling to the motion of N/S interfaces. While in the nonequilibrium state, the flux density can nearly equilibrate with the transient applied field, as determined by the amplitude of the signals. The solid lines in Figs. 2(a) and 2(b) are the fits used to extract these time constants, according to

$$M_{\text{probe}}(t_{\text{pump}}) \propto \int_0^{t_{\text{probe}} - t_{\text{pump}}} e^{-t'/\tau} H(t' - t_{\text{pump}}) dt'.$$

Assuming the microscopic pattern of the intermediate state here to be similar to that which has previously been directly imaged [13], in which the shortest length scale characteristic of normal ($H = H_c$) or superconducting ($H = 0$) regions is of order $1 \mu\text{m}$, N/S interface velocities in the 10-m/s range are required to reproduce the observed time constants. This is consistent with what may be expected [3] given the measured normal-state diffusion constant for the magnetic field. Note that because the technique is stroboscopic in nature and requires averaging of typically 100000 events per data point, the flux patterns are not spatially resolved in these experiments and a focus spot size of $75 \mu\text{m}$ is used. The exponential time constant for flux penetration seen here is presumed to reflect the same phonon escape bottleneck found in earlier transport studies of the nonequilibrium state [10], and the time constant increases in a similar manner as the transition is approached [5] by increasing T/T_c or H_0/H_c . As the system returns to equilibrium the inter-

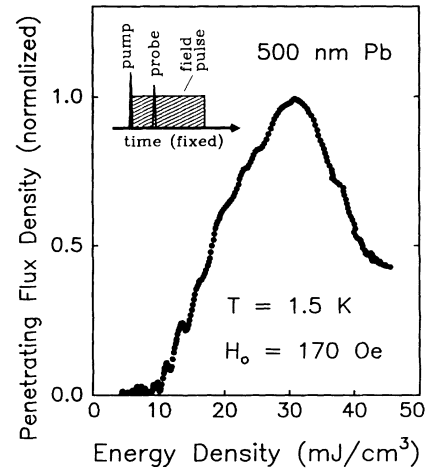


FIG. 3. The nonlinear pump power dependence of flux penetration through the nonequilibrium state, showing the onset threshold followed by a *nonmonotonic* evolution as the system is driven more strongly towards the normal state. 71-ns field pulse, 20-ns probe delay.

faces become pinned, leaving a flux arrangement which is frozen until the next pump pulse arrives.

Studies as a function of how far the superconductor is driven from equilibrium by optical pumping dramatically illustrate the unique flux dynamics of the nonequilibrium regime. The onset of the penetrating flux signal is observed at a well-defined pump threshold, above which the extent of flux penetration (for fixed time delays) actually evolves *nonmonotonically* as a function of pump intensity (linear response of the measurement system itself is confirmed by normal-state measurements). This is illustrated in Fig. 3 for a 500-nm Pb film at $T = 1.5 \text{ K}$, $H_0 = 170 \text{ Oe}$, where $70 \text{ mJ}/\text{cm}^3$ is the calculated energy density [16] to locally drive the film fully (electrons and phonons) above T_c . At some energy density well above threshold the signal starts to decrease, indicating that the efficiency of flux penetration begins to decrease as the illuminated spot is driven strongly towards the normal state, and the N/S interfaces are increasingly eliminated. The threshold pulse fluence for observation of the nonequilibrium signal in this work is significantly lower than values reported in transport studies [10,11]. The higher threshold powers found in the resistive measurements may be understood from the requirement in that case to drive the films sufficiently far from equilibrium to break any percolating superconducting paths along the current direction, whereas the magneto-optic sampling probe, more sensitive to the motion of normal/superconducting interfaces, allows us to study the dynamics of a less strongly perturbed nonequilibrium regime.

Another indication of how the flux dynamics are influenced by the equilibrium configuration of N/S interfaces is given in Fig. 4, where the screening response of the intermediate state is contrasted for parallel and per-

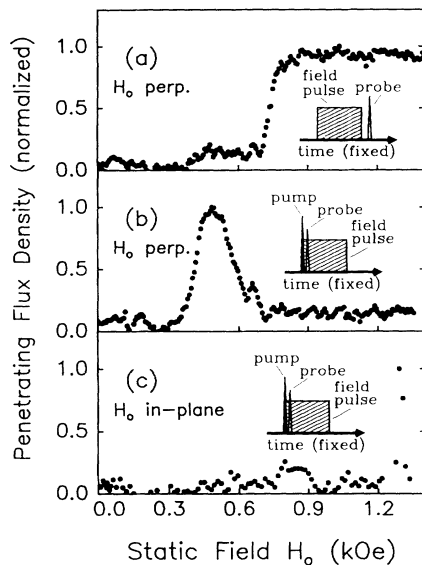


FIG. 4. (a) Screening response of a 500-nm Pb film at $T=1.5$ K, in the absence of a pump pulse, as a function of the perpendicularly applied static magnetic field. 71-ns-wide field pulses, probe delay 100 ns. (b) Illustration of the static field dependence of the nonequilibrium response in the perpendicular (demagnetization factor $n=1$) configuration. Probe delay 5 ns, pump energy density 10 mJ/cm^2 . (c) Counterpart of (b) with the sample rotated such that the static field is nearly in plane.

pendicular applied static fields. Figure 4(a) shows the "conventional" screening response observed when the magnetization is probed at fixed time delay in the absence of a pump laser pulse, as a function of the perpendicularly applied static magnetic field. The transition from complete screening by the superconducting film to a static-field-independent response in the normal state is not perfectly sharp, but is consistent with the value of the critical field determined by the low-frequency magnetotransport data on meander lines. Figure 4(b) shows the dramatically different [relative to Fig. 4(a)] static field dependence of the *nonequilibrium* response in the perpendicular (demagnetization factor $n=1$) configuration. These data show a peak at some position below H_c determined by a combination of the nonmonotonic dependence of Fig. 3 (which must have a counterpart as a function of reduced static field for constant pump energy density) and of the slowing down towards H_c found in Fig. 2. Finally, when the sample is rotated such that the applied static field is nearly in the plane (the Sharvin geometry, which tends to stabilize straight laminae of normal region [17]), the nonequilibrium signal *disappears* [Fig. 4(c)], with the exception of a narrow feature at the in-plane critical field (again coinciding with the transport value). This feature reflects some very slow behavior which appears to be al-

most time independent in the stroboscopic measurements.

In summary, direct measurements of flux dynamics in the optically induced nonequilibrium state of superconducting films have been reported. These experiments explicitly explore the important connection between studies of magnetic flux structures and of nonequilibrium effects in superconductors. The phenomenology of results obtained in the nonequilibrium regime indicate that the observed rapid flux penetration depends on the microscopic arrangement of normal/superconducting interfaces. A connection between the structure and dynamics arises in the theories of pattern formation in the superconducting transition [3], through the dependence of interface velocity on local curvature. A powerful feature of type-I superconductors as model systems for inhomogeneous kinetics is that the final structure towards which the nonequilibrium state evolves can be controlled by the strength and orientation of the applied static magnetic field.

Helpful conversations with D. D. Awschalom, C. C. Chi, D. P. DiVincenzo, R. J. Gambino, R. S. Germain, and G. Nunes, and assistance from M. J. Brady, A. M. Torressen, and R. R. Ruf, are all gratefully acknowledged.

- [1] R. P. Huebener, *Magnetic Flux Structures in Superconductors* (Springer-Verlag, Berlin, 1979).
- [2] P. Laeng, F. Haenssler, and L. Rinderer, *J. Low Temp. Phys.* **4**, 533 (1971).
- [3] H. Frahm, S. Ullah, and A. T. Dorsey, *Phys. Rev. Lett.* **66**, 3067 (1991); F. Liu, M. Mondello, and N. Goldenfeld, *ibid.* **66**, 3071 (1991).
- [4] L. R. Testardi, *Phys. Rev. B* **4**, 2189 (1971).
- [5] V. F. Elesin and Yu. V. Kopaev, *Usp. Fiz. Nauk* **133**, 259 (1981) [*Sov. Phys. Usp.* **24**, 116 (1981)].
- [6] D. D. Awschalom *et al.*, *Phys. Rev. Lett.* **55**, 1128 (1985).
- [7] M. R. Freeman, R. R. Ruf, and R. J. Gambino, *IEEE Trans. Magn.* **27**, 4840 (1991).
- [8] A. B. Pippard, *Philos. Mag.* **41**, 243 (1950).
- [9] R. P. Huebener, L. G. Stafford, and F. E. Aspen, *Phys. Rev. B* **5**, 3581 (1972).
- [10] C. C. Chi, M. M. T. Loy, and D. C. Cronmeyer, *Phys. Rev. B* **23**, 124 (1981); C. C. Chi (private communication).
- [11] X.-H. Hu, T. Juhasz, and W. E. Bron, *Appl. Phys. A* **52**, 155 (1991).
- [12] Mark Johnson, *Phys. Rev. Lett.* **67**, 374 (1991).
- [13] G. J. Dolan, *J. Low Temp. Phys.* **15**, 133 (1974).
- [14] H. Kirchner, *Phys. Status Solidi A* **4**, 531 (1971).
- [15] M. D. Maloney, F. de la Cruz, and M. Cardona, *Phys. Rev. B* **5**, 3558 (1972).
- [16] R. J. Corruccini and J. J. Gniewek, *Natl. Bur. Stand. Monograph No. 21* (U.S. GPO, Washington, DC, 1960).
- [17] Yu. V. Sharvin, *Zh. Eksp. Teor. Fiz.* **33**, 1341 (1958) [*Sov. Phys. JETP* **6**, 1031 (1958)].